AI-AEC-13080

ZIRCONIUM HYDRIDE REACTOR CONTROL DRIVE ACTUATOR DEVELOPMENT SUMMARY REPORT

AEC Research and Development Report

Atomics International Division
Rockwell International

P.O. Box 309
Canoga Park, California 91304

DISCLAIMER

NOTICE

AI-AEC-13080
SNAP REACTOR
SNAP PROGRAM
M-3679-R69
C-92b

ZIRCONIUM HYDRIDE REACTOR CONTROL DRIVE ACTUATOR DEVELOPMENT SUMMARY REPORT

L. E. DONELAN

Atomics International Division
Rockwell International

P.O. Box 309
Canoga Park, California 91304

CONTRACT: AT(04-3)-701
ISSUED: JUNE 30, 1973

DISTRIBUTION

This report has been distributed according to the category "Systems for Nuclear Auxiliary Power (SNAP) Reactor – SNAP Program," as given in the Standard Distribution for Classified Scientific and Technical Reports, M-3679.

CONTENTS

TABLES

FIGURES

ABSTRACT

Over the years, actuators for compact space nuclear reactor reflector control have progressed from modified commercial units with relatively short life and low reliability at moderate temperature, to units custom designed for specific application. These latter units have demonstrated long life and high reliability at high temperatures. The design for a specific application now includes the ability to design for various torque and step sizes, and the ability to control the relative proportions (length and diameter) of the actuator. The present status of design calculation capability incorporates reliable computer programs to facilitate the design and selection of the actuator, in the form of:

1) A stepper motor program to calculate actuator performance based on physical configuration

2) An actuator brake program to calculate the magnetic performance based on a physical brake configuration

3) A bearing program to calculate loads and clearances for initial end bell and bearing interferences and journal dimensions.

Using the preceding programs and various other supporting calculations, a control drive actuator has been designed for the 5-kwe Reactor Thermoelectric System, to fit in the available space within the reflector and shield configuration. This actuator will develop sufficient torque for both the specified stepping drive control and the scram requirement, at current densities no greater than the proven SNAP 8 Developmental Reactor design.

The report contains a brief history of the progress of actuator design, development, and tests to date, as well as the design calculations applicable to the actuator designed for the 5-kwe Reactor Thermoelectric System.

BLANK

I. INTRODUCTION

A series of compact nuclear reactors and electrical power systems were designed, developed and tested for the Space Nuclear Auxiliary Power (SNAP) program. The zirconium hydride (ZrH) reactors for these systems were fueled by hydrided zirconium uranium elements. Windows in the external beryllium neutron reflector were adjusted by rotating drums or by sliding segments to regulate neutron leakage from the core and thus the power output of the reactor. A direct radiating thermoelectric module Power Conversion System (PCS) produced over 500 watts of electric power in the flight-tested SNAP 10A system. Mercury-Rankine cycle turbogenerator PCS's of 3 kwe and 30 kwe power range were demonstrated for the SNAP 2 and SNAP 8 systems respectively. The latest 5-kwe Reactor Thermoelectric System design was based on the use of a compact, tubular thermoelectric PCS. The NaK, used to transfer the heat from the reactor to the PCS, and from the PCS to the space radiator, was circulated by dc conduction electromagnetic (EM) pumps on the thermoelectric systems, and by mechanical centrifugal pumps on the Mercury-Rankine systems.

A. FUNCTION

The control of SNAP reactor systems is accomplished by varying the number of neutrons that are allowed to escape through an external reflector. An opening in the external reflector acts like a window, the size of which can be changed by changing the effectiveness of reflection. In the SNAP 10, SNAP 2 and S8DR type of reactors, neutron reflector control was effected by use of cylindrical sections having reflector material in one portion and a void on the balance. These sectors were rotated by a reflector drive actuator through a gear. In the 5-kwe Reactor Thermoelectric System reflector control was accomplished by linearly displacing two movable control sectors in the reflector assembly. A ball screw was utilized for converting rotary motion to linear motion. Although the movable reflector configuration, i.e., linear versus rotary displacement, was different from previous reflector designs, the actuator employed was a direct extension of previous designs.

B. BASIC DESIGN CONCEPT

1. Design Criteria

The basic requirement of a reflector control actuator is to provide a small incremental motion of sufficient energy to reposition the movable reflector. This must be done both at ground test conditions and in expected space environments. The total environment includes ambient and elevated temperature, radiation, ambient and space pressure (vacuum), launch vibration, shock and acceleration loads.

The specific design criteria varied from actuator to actuator, generally with an upward trend in performance requirements with time. A list of the various actuators on which development was performed, and the required torques, operating temperatures and position accuracy are shown in Table 1.

TABLE 1

ACTUATOR PERFORMANCE CRITERIA

Reactor System	Actuator Torque (oz-in.)	Actuator Position Accuracy (degree)	Max. Temp. (°F)
SNAP 10A	12	~	650
SNAP 2 DRM-1	20	~	950
SNAP 8 DRM	20	~	950
SNAP 8 DS	37	0.412	1000
SNAP 8 DR	37	0.412	1000
SPF	52	0.60	1000
ZrH	170	0.70	1000
5-kwe Thermoelectric	100	0.6	800

Other design criteria included maximum reliability, minimum power requirements and minimum weight.

2. Design Concept Selection

Various types of drives capable of providing small incremental rotary motion were originally considered. These concepts included spring and

escapement mechanisms, hydraulic drives, small high-speed motors and high-ratio gear drives, as well as stepper motors. Straight mechanical devices were rejected because of a limitation on the total available number of steps and low inherent reliability due to lubrication problems. High-speed motors and gear reducers did not appear attractive since gear and bushing lubrication problems at high speed were expected to impose severe problems at high temperatures in a vacuum under irradiation. Hydraulic drives did not appear feasible because of the limitation of available radiation-tolerant hydraulic fluids, mechanical problems, and problems associated with obtaining accurate and repeatable step displacements.

On the other hand, stepper motors were commercially available which did not require brushes or commutator bars, incorporated a simple bearing structure, utilized a simple winding design in the stator only, and provided small stepwise motion. Commercially available windings and bearings, however, would not meet the temperature, radiation and pressure requirements. Also, a method was required of preventing the actuator shaft from rotating, when not stepping, without continuously applying current.

The initial design concept was to utilize the stepper motor principle and commercial parts where possible, but develop high-temperature, radiation-resistant windings and bearings, and add a brake. The unit also had to be radiation hardened. This concept is illustrated in Figure 1. The stepper motor contains a wound stator assembly of eight slotted pole pieces (a total of 48 teeth). The rotor, containing a permanent magnet, is slotted in a similar manner, but contains 50 teeth. Sequential energization of the bifilar wound stator coils causes the field to rotate, which, by the reluctance principle, generates a torque in the rotor until a half-tooth pitch motion has taken place, at which time the torque is reduced to zero. Based on the geometry selected, each step results in a motion of 1.8 degrees. Physical alignment of the rotor is obtained by sleeve bearings located in the end bells, using selected fits on the poles and stator shells. The journals contain flame-sprayed, alumina-oxide coated shafts, ground to size, which operate in a carbon graphite sleeve sized to remain tight in its housing at operating temperatures.

The EM brake is an energized-to-release device. When the brake coil is energized, the armature (stationary brake disk) is pulled to the brake face by

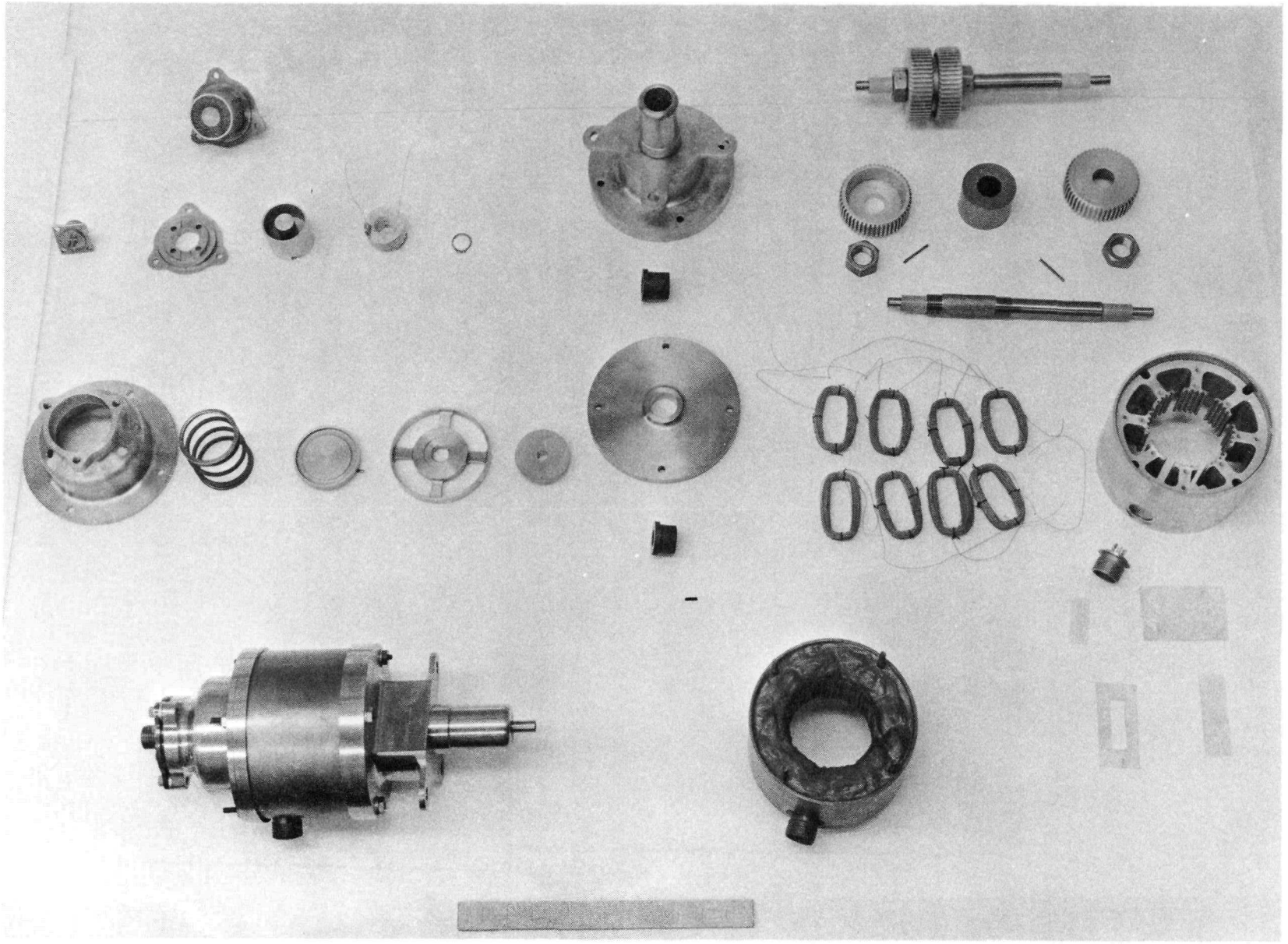

7550-5556G

Figure 1. Indirect Drive 1.8-Degree Step Actuator Assembly and Components (SNAP 10A)

the magnetic flux, releasing the disk engagement and allowing the rotor and brake disk to rotate. With deenergization, the plates are forced into engagement by the spring force built into the brake assembly, locking the actuator from further rotation.

In actual operation, positional control is obtained in the actuator by control of the electrical pulse train. The first phase of the stator is energized prior to the brake being energized, thus holding the stepper from rotating. After the proper number of pulses to the various phases to achieve the desired rotation of the stepper, the brake is deenergized, and allowed to lock, prior to the deenergization of the last stepper pulse. Under the above conditions, the rotor is always under positive control and never free to drift.

II. ACTUATOR EVOLUTION

Over the years, starting from the initial design concept, several generations of actuators have been designed, developed, and built to control reactor movable reflectors. These actuators, as listed previously, have been identified by the reactor system for which they were designed.

A. DESIGN DESCRIPTION AND FEATURES

In general, the actuators that have been used in reactor control are all of the variable reluctance EM type. These EM devices were of the pulsed-dc design with a built-in brake. Although only one basic type of actuator was used on the reactors, many alternate designs were considered and carried through testing. The first actuator developed was used on the SNAP 10A reactor.

1. SNAP 10A Actuators

At the start of the SNAP 10A program, commercially available actuators of the type desired that would function reliably for 10,000 hr in a space environment were not available. The high neutron and gamma flux, the high steady-state temperature and temperature gradients, and the high vacuum of outer space required new technology in rotary actuator design. The SNAP 10A actuator was thus basically a commercial stepper motor with various modifications as follows:

1) An attached brake was added to the stepper motor connected in series with the windings.
2) Chrome plating was added to the lamination material (AISI type M-36 with black iron oxide).
3) The bifilar winding was replaced with a high-temperature winding and insulating system (copper, glass, mica and commercial ceramic type cement).
4) The end bells and bearings were replaced with a high-temperature design (titanium and carbon graphite).
5) The shaft and bearing journals were replaced (titanium and aluminum oxide).

This actuator, assembly and exploded view, is illustrated in Figure 1. The rotor assembly includes an Alnico permanent magnet.

The rating of the SNAP 10A actuator was a modest 12 oz-in. stepping torque at 650°F, but it performed the required operations satisfactorily.

2. SNAP 2 DRM-1 and SNAP 8 DRM Actuators

This generation of actuators utilized a solid rotor (Figure 2), an improved design of the SNAP 10A actuator. Several other design changes were made in the rotor, stator, and brake. The rotor was a one-piece unit with the permanent magnet eliminated. The rotor slots are milled "in-line" in contrast to the SNAP 10A actuator, in which the slots were misaligned by one-half the pitch of the slot. These changes enabled the rotor to operate more reliably at the higher temperature and also eliminated many parts such as end caps, hold-down units, lock pins, etc., thus making manufacturing easier and less costly. The end result was a lighter, more accurate, and more reliable rotor assembly.

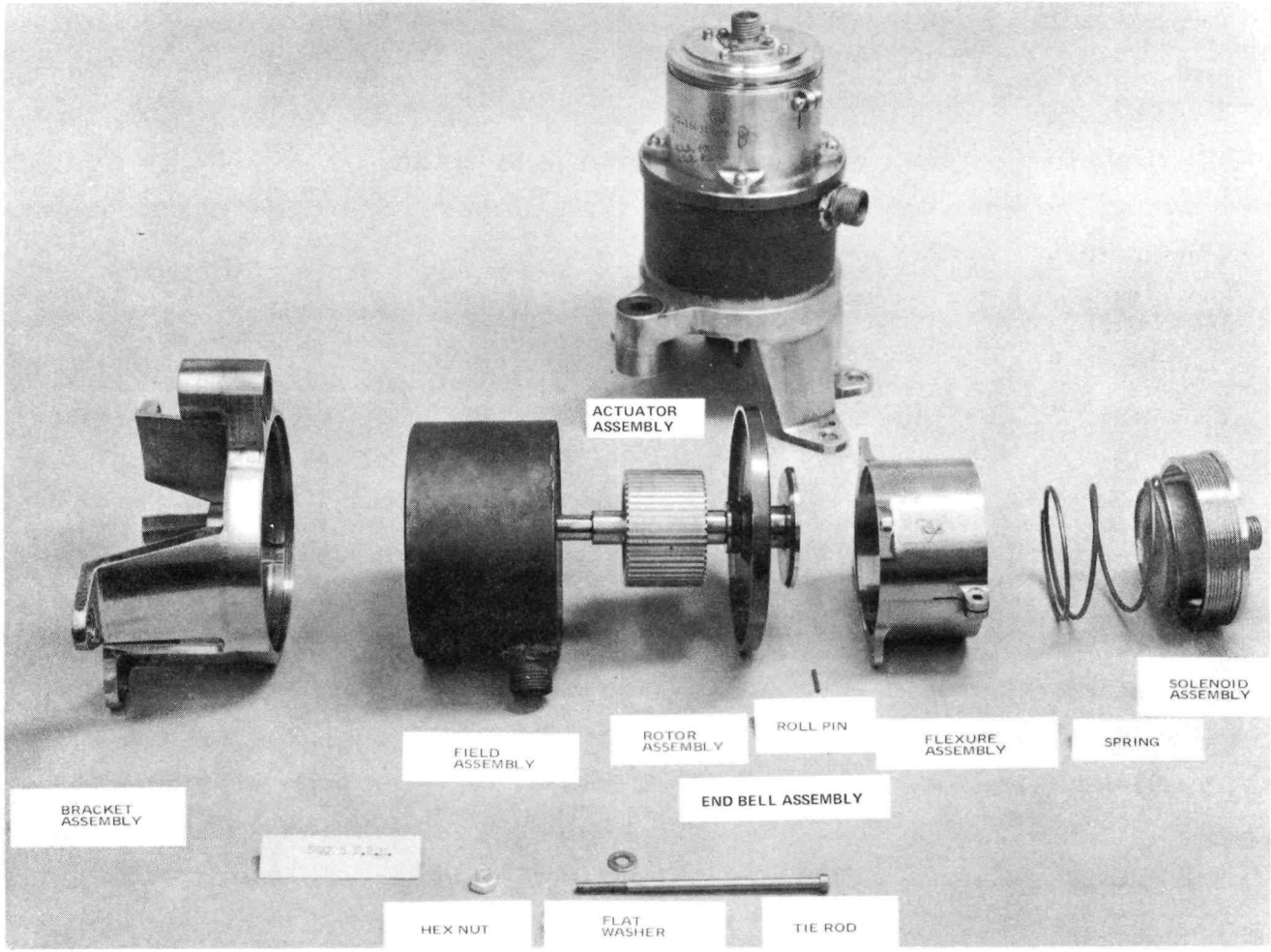

7573-1061A

Figure 2. Indirect Drive 1.8-Degree Step Solid Rotor Actuator (S2DRM-1 and S8DRM)

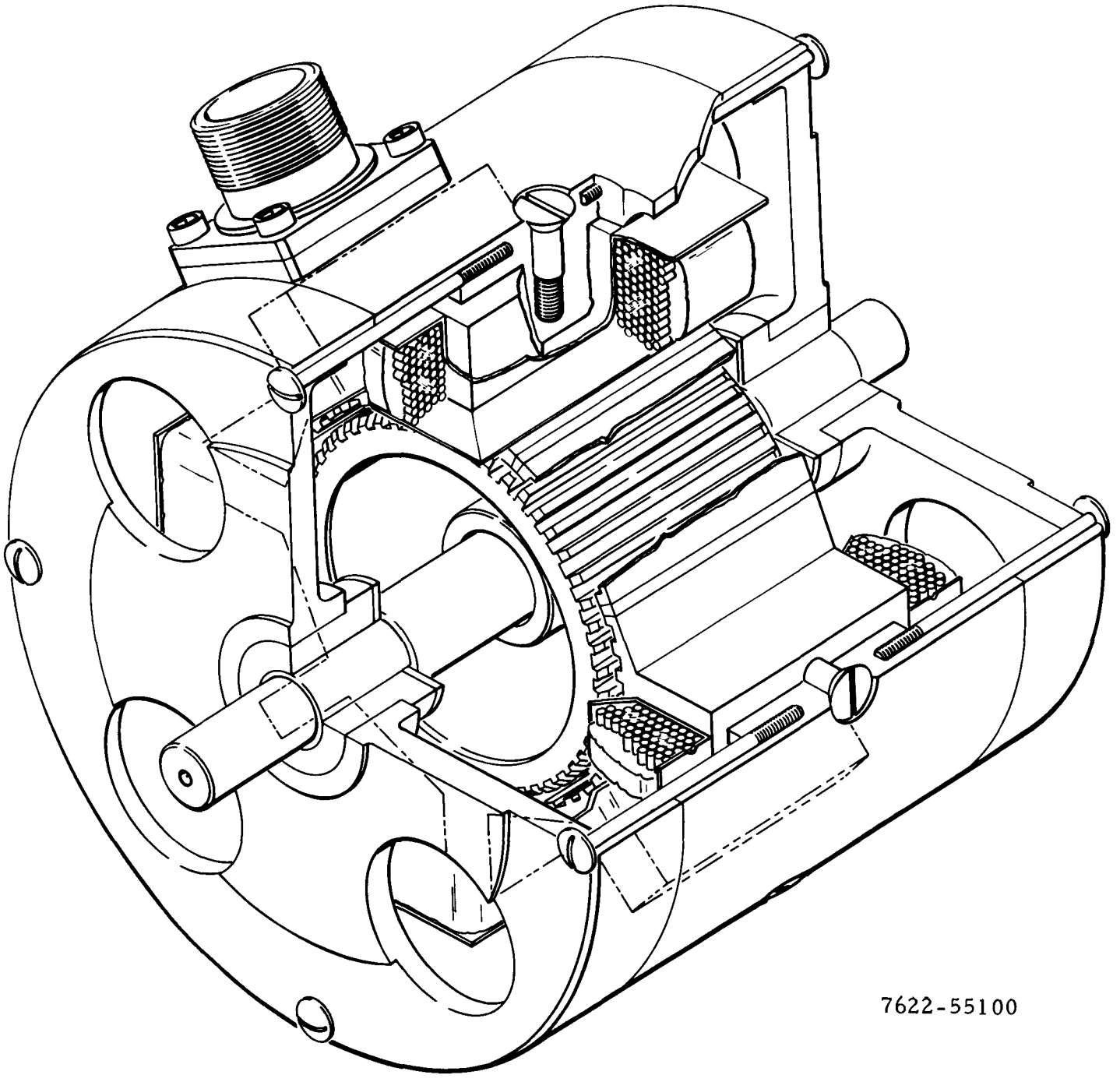

Figure 3. Indirect Drive 1.8-Degree Step Actuator (S2DRM-1 - S8DRM Backup)

The stator was changed from a bifilar winding with two coils per pole, as in the SNAP 10A actuator, to a single winding with one coil per pole. The conductor was changed from copper to chrome-plated copper wire. Since more gross copper was used, the heating losses and power consumption were reduced.

The brake was redesigned and incorporated a wet-wound* technique. It also had a new type of flexure member and optimized design configuration to meet the applicable requirements.

In general, the solid-rotor produced more torque (20 oz-in. at 950° F), had a greater step accuracy, and higher reliability at lower power consumption than the SNAP 10A actuator.

Backup Actuator Designs

A backup actuator design for the S2DRM-1 and S8DRM actuators is shown in Figure 3. This actuator was similar to S2DRM-1 and S8DRM except that the stator was "solid" (machined) rather than being made from a lamination stack and was designed to accept wet-wound stator coils. These coils were inserted over the poles prior to the poles being inserted into the stator shell. With this method of fabrication the design performance was improved as well as reliability. This was due to the increased quality of the prefabricated wet winding. This design had improved performance but development was not completed in time to be used on the system. However, the experience gained was used in the next generation of actuators.

A direct drive 0.5-degree stepper motor was designed as an alternate for the SNAP 2 and SNAP 8 systems, as shown in Figure 4. This device was essentially a reluctance stepper which took a 0.5-degree step per pulse. The decreased step size was obtained by increasing the rotor diameter to near the maximum machine diameter and using a double magnetic gap per pole. This eliminated the need for a gear train. The output torque of this design was much lower than predicted. This was later determined to be due to an adverse magnetic gap-to-tooth-width size ratio.

*Wet winding is the technique of applying a liquid ceramic cement to the wire as it is wound into a coil. The coil is subsequently oven-cured to solidify the insulation system.

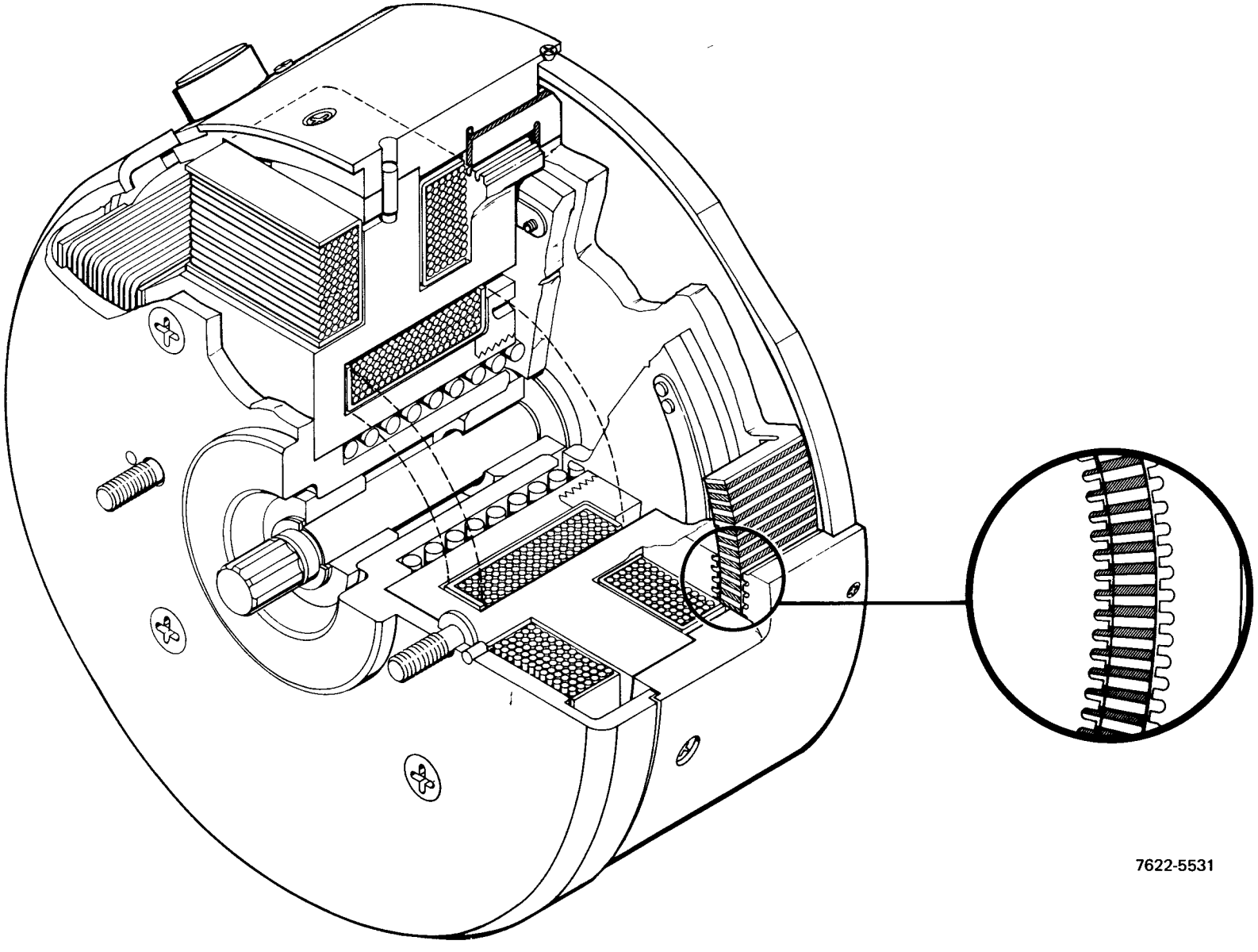

Figure 4. Direct Drive Electromagnetic 0.5-Degree Stepper – Model 3

Still another backup actuator was the Linear Actuator depicted in Figure 5. This device utilized frictional contact points to the outer rotatable drum, in conjunction with a solenoid-actuated movable segment to achieve motion. Adjustable stops regulated the degree of motion per step sequence. Difficulty in adjustment, slippage, and high unit loading, which were conducive to self-welding, were deficiencies of this design which caused it to be dropped.

3. S8DS, S8DR, SPF, ZrH Actuators

The S8DS system was the first actuator of the next generation. These actuators incorporated all of the improvements in design features gained from previous development, with several additional improvements. This generation of actuators was required due to an increase in torque requirements of the new generation of reactors and of the reflector control system. The major improvements consisted of fabricating all the structural parts, including the rotor, of the same material; thus, differential thermal expansions were reduced and more "working" iron was provided. The working iron material was an alloy of 27% cobalt and 73% iron, selected for its high-temperature magnetic characteristics. The rotor and stator teeth were machined with the same tooth pitch, with all teeth of a phase providing maximum torque at the same value of rotor angular displacement. This alignment is illustrated in Figures 6 and 7. A chip guard was placed under the encapsulated coil and bobbin as a shield to prevent dirt or insulation dust from collecting between the rotor and stator teeth or reaching the bearings.

The brake surfaces utilized the same iron material with teeth machined to match during engagement. The mating surfaces were coated with colloidal graphite and MoS_2 to inhibit self-welding. An exploded view drawing is shown in Figure 8.

The S8DR actuator after acceptance testing is shown in Figure 9. This actuator had the following additional improvements not contained in the S8DS actuator:

1) The lead cable was connected directly to the coils, increasing reliability by elimination of the connectors, which had a failure history.

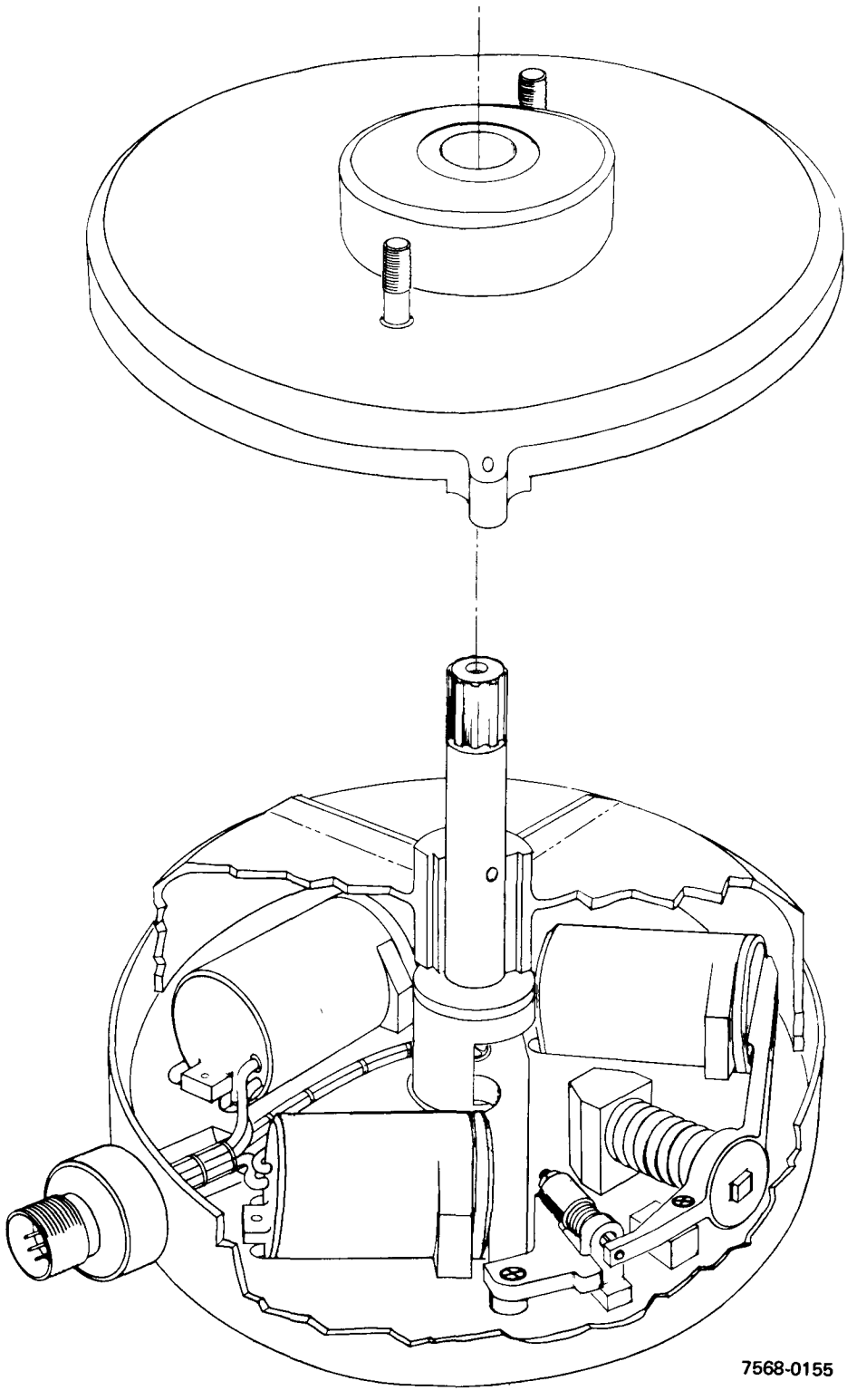

Figure 5. Linear Actuator (SNAP 2 – SNAP 8 Backup)

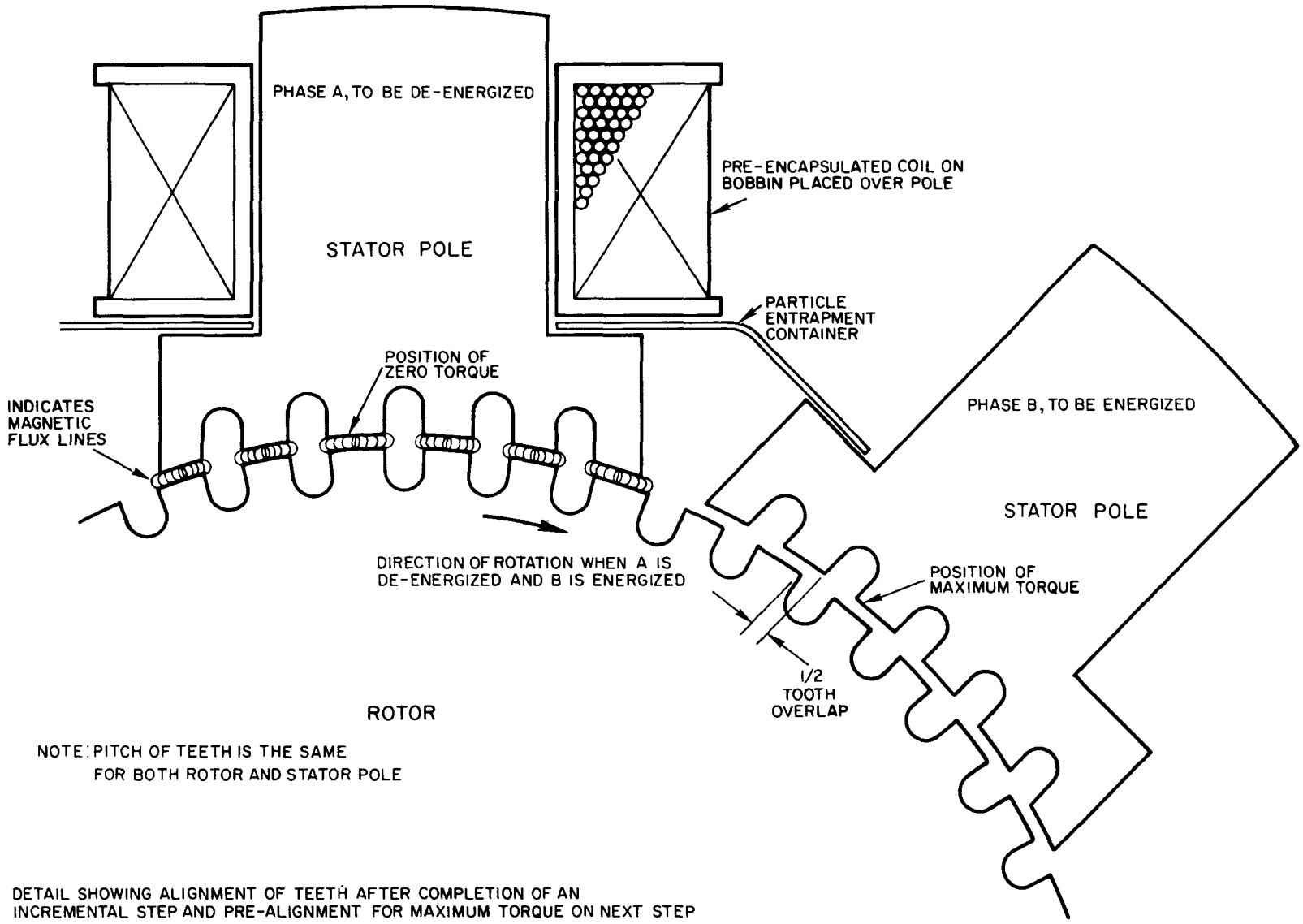

Figure 6. Tooth Alignment

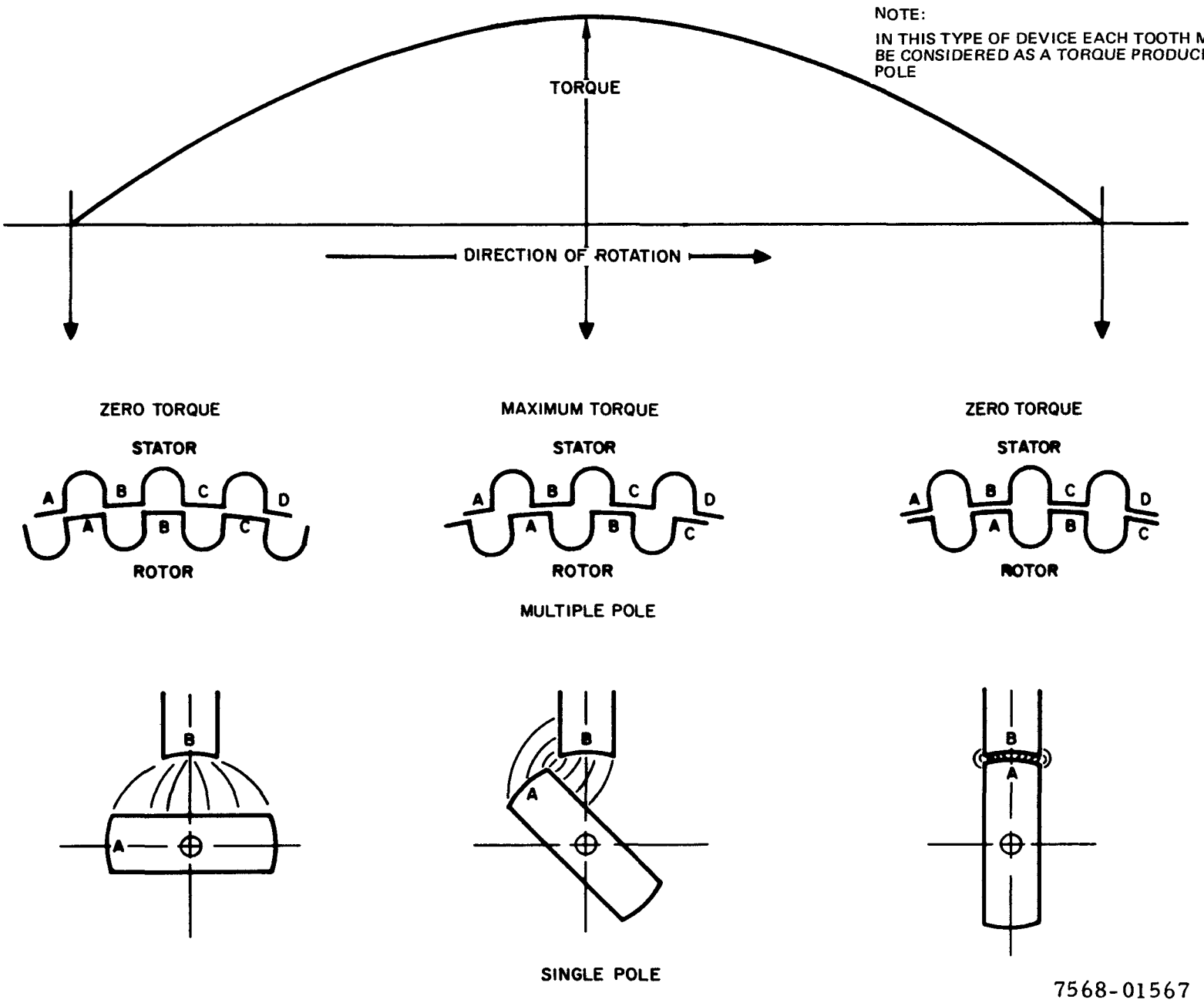

Figure 7. Stepper Motor Principle of Operation

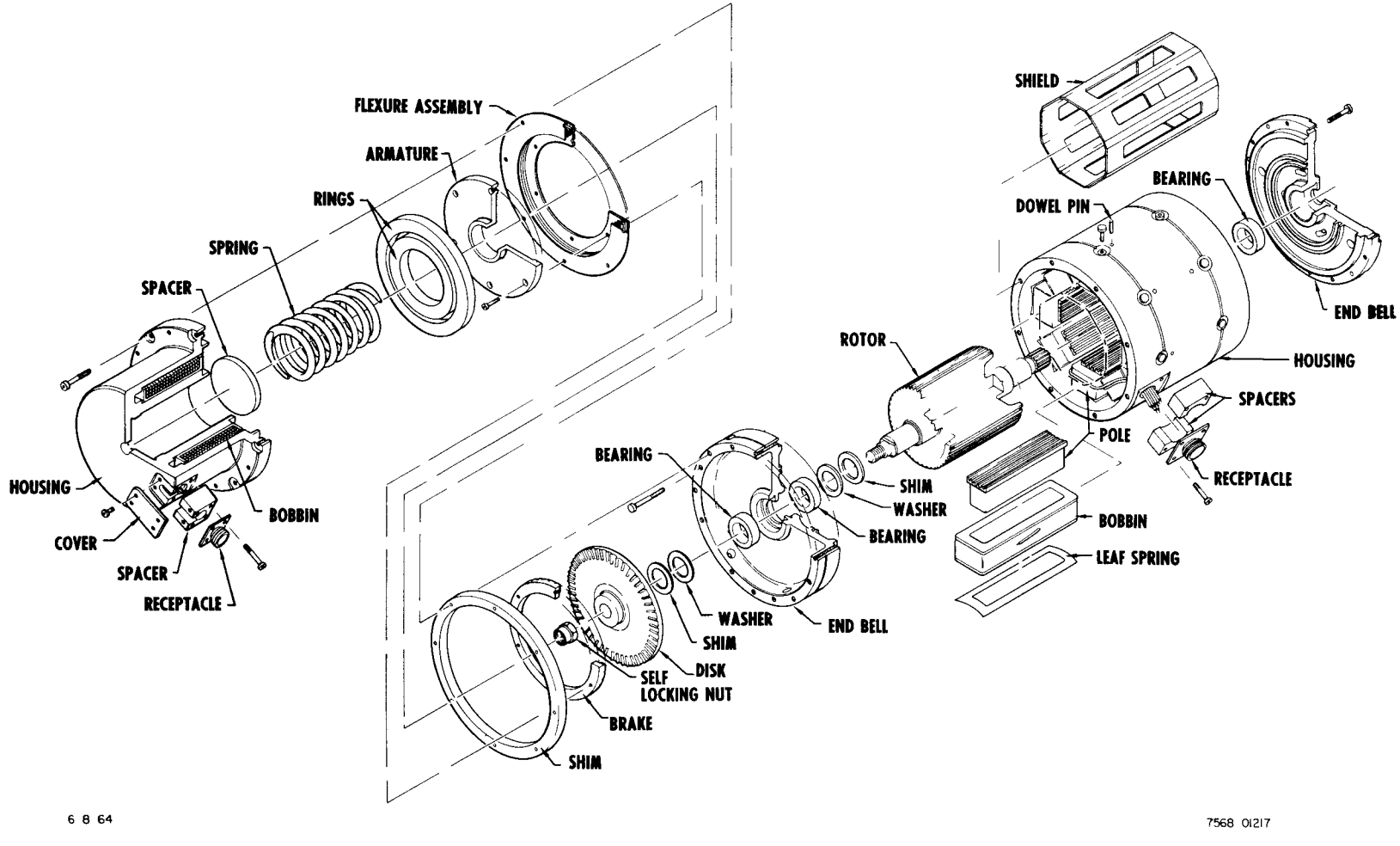

Figure 8. 1.8-Degree Stepper Motor 8DS Model - Exploded View

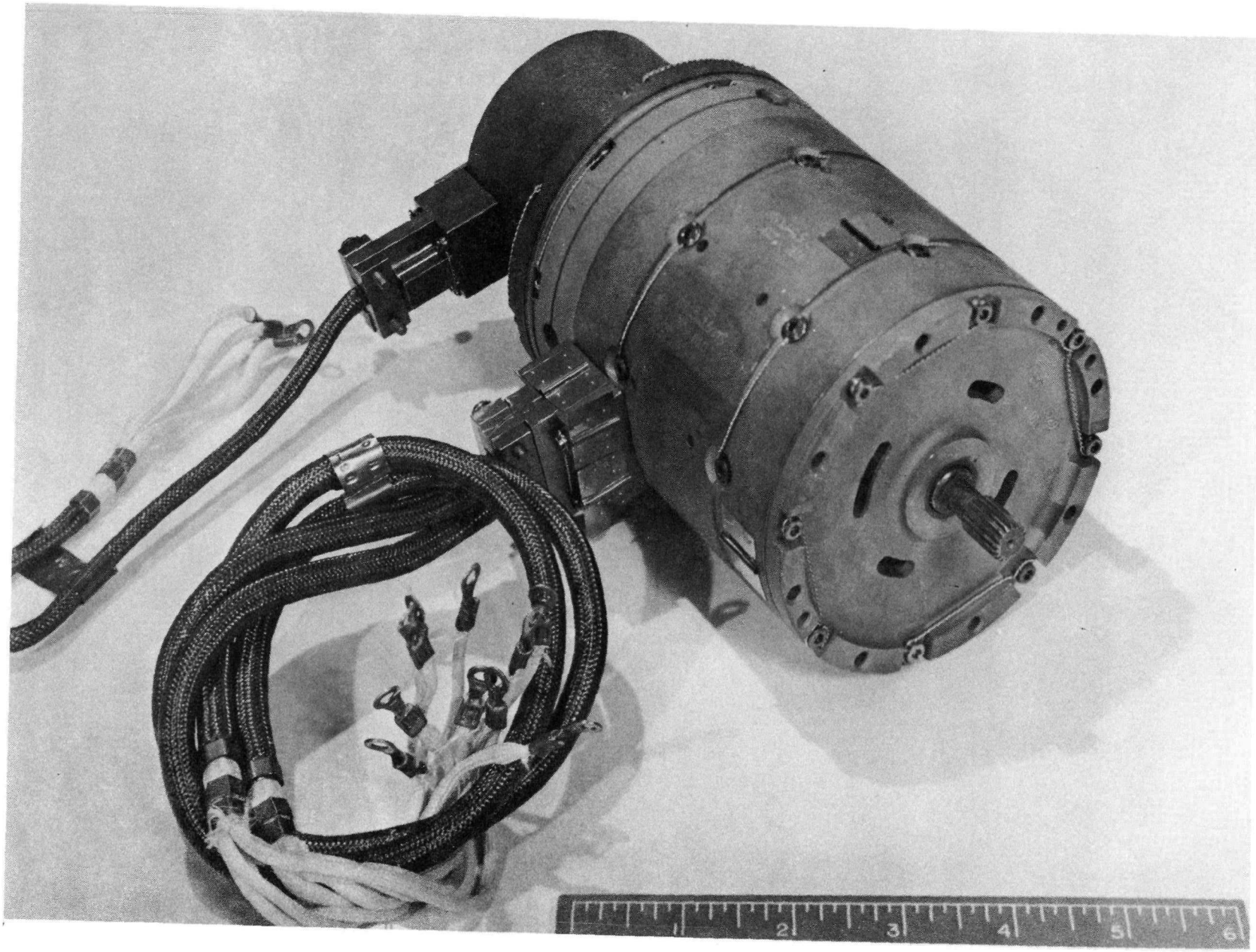

Figure 9. S8DR Actuator After Acceptance Testing 7695-55516

2) The conductor wire was changed from chrome plated copper to stainless clad copper.

3) The stepper coils were connected in parallel rather than series.

These improvements were also included in the SPF and ZrH actuators. Although there was one basic actuator, it had a different rating for each application (Table 2), based upon wire gage used, duty cycle, and previous test data obtained.

TABLE 2

ACTUATOR OPERATING CHARACTERISTICS

Parameter	Reactor		
	S8DR/S8DS	SPF	ZrH
Dynamic torque (oz-in.)	37	52	170
Load error (deg)	0.412	0.60	0.7
Positional torque (oz-in.)	20	42	150
Holding torque (oz-in.)	88	80	240

With the increase in torque required from the actuator over the DRM series, a larger envelope was allowed, which accommodated an improvement in bearing design and allowed the thrust surfaces to be mounted adjacent to each other. This facilitates rotor axial positioning and is especially valuable in accommodating thermal transients and differential temperatures. These actuators were 4-1/8 in. in diameter, 8-3/8 in. long, and weighed 15-3/4 lb.

The latest actuator to be designed, for the 5-kwe thermoelectric system, is discussed in detail in Section III.

B. PERFORMANCE OF ACTUATORS

After the actuators were designed, engineering models were made to test the various components, such as coils, bearings, and construction features. The results of these tests were factored into the design of developmental actuators which were prototypes of the reactor system actuators. Testing of these units established the acceptance test requirements. In general, the developmental actuators were used as the qualification test actuators.

1. Reactor System Actuators

Actuators were used in reactor operation both in ground testing and in flight service. The following is a summary of the successful operation of actuators in a reactor system:

SNAP 10A Ground Test	2 Actuators	10,000 hr
SNAP 10A Flight	2 Actuators	46 days
S8DR	6 Actuators	6,400 hr

2. Development and Qualification Actuators

Actuator developmental and qualification testing is summarized in the following subsections. In general, the tests were successful and information obtained in the testing allowed not only for the establishment of the acceptance test requirements of the system actuators, but also established the requirements and changes necessary for more reliable units to operate with greater torques at higher temperatures.

a. SNAP 10A

A total of 27 actuators were made and tested for a total unit test time of 90,600 hr. The maximum unit test was 11,400 hr. Five actuators were life tested for 9,000 hr and 60 thermal cycles each, while two actuators were radiation tested at 1.8 to 5.5 x 10^9 R and 1 to 5 x 10^{18} nvt > 0.1 Mev. Other units were shock and vibration tested as well as being tested for engineering evaluation.

b. SNAP 2 DRM-1 and SNAP 8 DRM

The modification to these actuators for the higher torque and temperature was relatively minor; but to evaluate the modification, 7 units were made and tested for a total of 20,000 hr at 1000° F. Due to mounting changes, shock and vibration testing was performed on this design. Radiation testing was not rerun, as all the materials of construction had been proven in the SNAP 10A radiation tests.

c. SNAP S8DS and S8DR Actuators

The latest actuators tested were of the S8DS and the S8DR design. These actuators performed to the requirements of the specification. The following is a summarized tabulation of the testing:

Actuator	S8DS	S8DR
Actuators, developmental	15	3
Total test time (hr)	83,000	53,581
Test temperature (° F)	1025	1125
Shock and vibration	Yes	No
Radiation	Yes	No

One of the S8DR units was tested for over 20,000 hr without malfunction.

3. Component Tests

Component tests were performed on various items to determine the most suitable materials and processes. Although all items of the actuator were tested, some of the most significant results are presented in the following subsections.

a. Coil Testing

Coil testing was performed on both material and construction. The most reliable construction (and the reference design) was found to be a wet-wound coil of stainless steel clad copper, with built-in lead wire of this same material, wound on an alumina bobbin. Other materials tested were:

1) Dispersion hardened copper

2) Nickel clad silver

3) Copper

4) Chrome plated copper.

One very important factor in the selected coil design was that there had never been a catastrophic failure of a reference design coil, i.e., stainless steel clad copper.

b. Bearing Tests

Tests were performed on suitable bearings. This testing and results form the basis of a separate summary report.*

c. Structural Fabrication

A number of tests were performed on the method of fabrication including welding, brazing, and bolting. The most satisfactory structure was found to be one machined from one piece of bar stock and bolted together, with special attention given to thermal expansions.

4. Materials Testing

Materials evaluated by testing for suitable magnetic qualities were:

1) 27% cobalt iron

2) Pure iron

3) Silicon irons.

The most suitable material, as regards magnetic properties at high temperatures, was the 27% cobalt iron. It was also sufficiently ductile for fabrication by the selected methods. Care was required, however, due to a somewhat brittle nature at ambient temperature.

5. Subassemblies Testing

The subassemblies of the stator of the stepper motor and the brake assemblies were also tested. This was generally done before, or in conjunction with, the building of the developmental actuators. Test duration was normally only a few hundred hours, although some tests were conducted for up to 15,000 hr.

---

*P. H. Horton and W. J. Kurzeka, "Zirconium Hydride Reactor Control System Bearing Development Summary Report," AI-AEC-13079 (June 1973)

III. 5-kwe REACTOR THERMOELECTRIC SYSTEM ACTUATOR

A. DESIGN REQUIREMENTS

The last actuator designed was for the 5-kwe Reactor Thermoelectric System. It was designed to meet the increased output requirements and to conform to the allowable space. This design is a logical extension of the S8DR actuator. The first stage of gearing is included within the actuator envelope. This configuration is shown in Figure 10.

1. Performance

The performance requirements of the actuator, as measured at the input to the first stage of gearing, are as follows:

Output step size	7.2 degrees (4 pulses of 1.8 degree)
Scram torque (6 rpm)	70 oz-in., minimum
Stepping torque	100 oz-in., minimum
Brake torque (holding)	180 oz-in., minimum
Lifetime	
Hours	44,000 minimum
Thermal cycles	50 (50° F to 800° F)
Operational cycles (step rate)	50,000 steps in each direction

The environmental requirements, in addition to normal handling, shipping, and storage, include launch acceleration and vibration, as well as high-temperature (~ 800° F) high-vacuum operation. The design requirements resulted from the reflector and actuator drive conceptual studies. Various arrangements of the reflector drive and actuator components were studied simultaneously to determine the most suitable overall configuration. As each arrangement of the reflector drive gave a different torque and step requirement, so did each actuator arrangement produce a different torque and step capability. Basically, this study resulted in an energy control system. The study rapidly pointed up the need for the actuator to develop an increased energy capability per step.

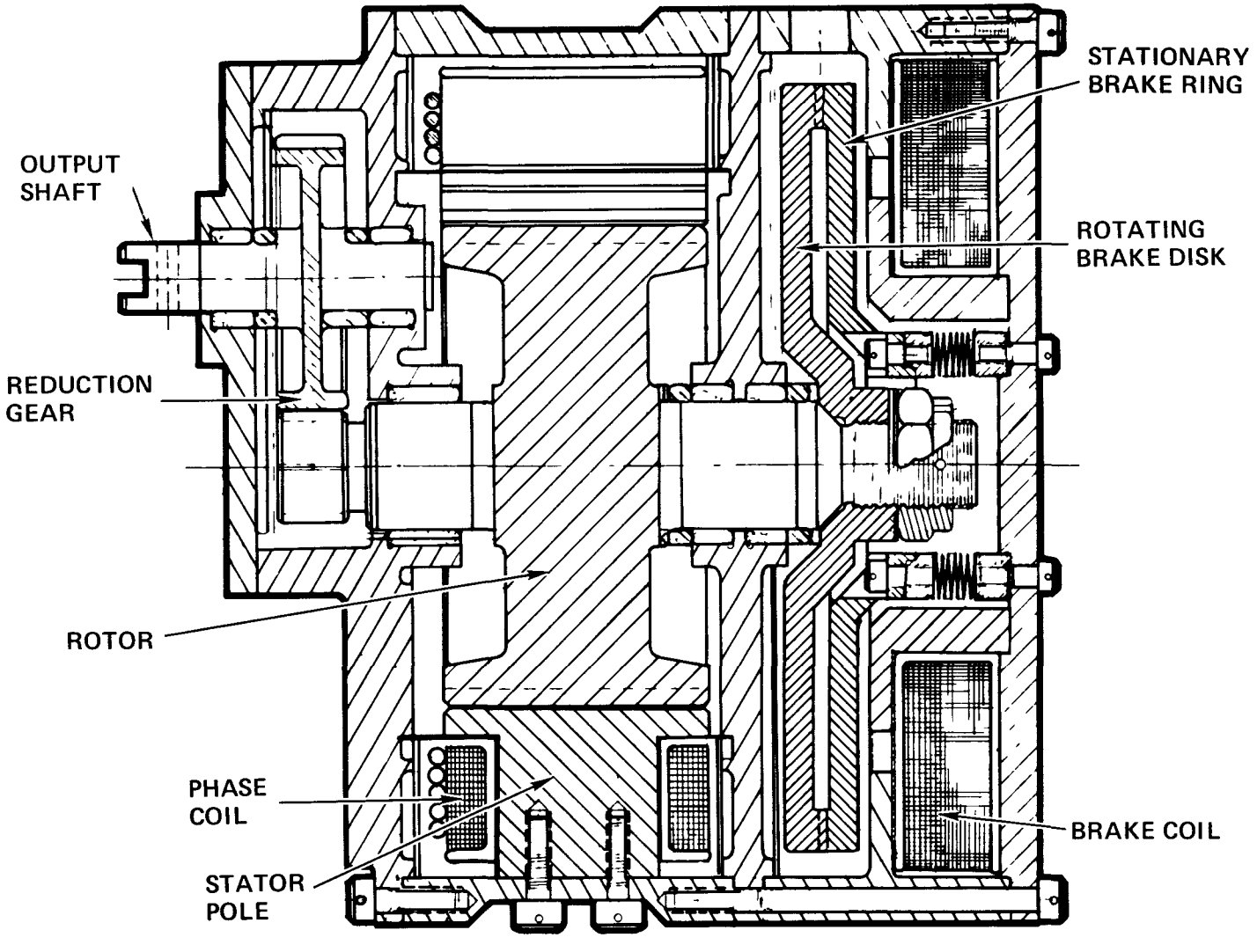

Figure 10. Control Drive Actuator

B. DESIGN OPTIMIZATION STUDIES

From previous experience, it was expected that an increased energy capability per step would require an increase in overall machine volume due to an increased flux requirement, or to accommodate an increased motion of the torque-producing elements. The conceptual reflector studies established a maximum diameter and the desirability of a short actuator length. This established the actuator diameter for the studies. With the increase in outside diameter, the rotor diameter could be increased, which would allow for an increase in the number of teeth or an increase in tooth size, since there is a finite ratio between tooth size, number of teeth, and diameter.

Also factored into the selection of the design, in addition to the requirements of torque and size limitations, was the requirement to use design parameters as established by the performance of the S8DR actuator. This included not only limitations on the material working levels, such as current density, but also test-proven methods of calculation. Any extensions of the parameters or levels had to be proven by testing.

Experimental data obtained in the past was reevaluated by use of a computer code prepared to calculate the performance of an actuator from its physical size. The main problem encountered was the evaluation of the equivalent flux leakage path between teeth at the point of maximum torque. Various analytical models were checked with the assistance of the computer until a reasonable correlation with the 0.063-in.-wide slots (as used in the S8DR design) was obtained, as well as with the smaller 0.040-in.-wide slots. With the aid of this program, an extrapolation to larger teeth was performed. This extrapolation, as well as an evaluation of machines with smaller teeth, indicated the desirability of larger teeth in the actuator for the 5-kwe system.

To verify the computer code ability to calculate the larger tooth actuator performance, a test assembly of S8DR developmental parts, with replacement poles having larger teeth, was made and tested. The additional information obtained, verified the computer program.

1. Analytical Calculations

A stepper motor, Figure 10, is a permeance machine; that is, its output energy is derived from a change of permeance with physical motion of the shaft. A permeance machine* will produce torque in accordance with the following formula:

$$T = K\,NI^2\,\frac{dP}{d\theta}$$

where

T = static torque (oz-in.)
K = a constant to accommodate units
NI = magnetomotive force (ampere turns)
$\frac{dP}{d\theta}$ = differential permeance with angular motion .

The problem arises in the evaluation of the differential permeance. This is compounded by the stepper having two types of permeance change with the shaft motion: (1) that of the magnetic gap, and (2) that of the materials of construction, due to changing flux levels.

Because it was intended to calculate the performance of a stepper motor from its physical size, the permeance formula was converted to a more convenient form as follows:

$$T = K\,L\,N\,R\,(B_1^{\,2}\,G_1 - B_2^{\,2}G_2)$$

where

T = static torque (oz-in.)
K = constant to accommodate units
L = axial length of teeth (in.)
N = number of working teeth
R = radius of rotor gap (in.)
B_1 = flux density maximum in gap ($KL/in.^2$)
G_1 = magnetic gap rotor to stator (in.)
G_2 = equivalent leakage gap (in.)
B_2 = equivalent leakage gap flux ($KL/in.^2$)

*H. C. Roters, Electromagnetic Devices, (John Wiley & Sons, Inc., 1941)

The above formula neglects the change in permeance within the magnetic material. This omission was based upon the consideration that the net change in flux density within the magnetic material for an infinitesimal motor movement would result in a neglectable permeance change of the actuator; and, therefore, the only permeance change to be considered is that of the gap. Subsequent testing verified this assumption.

All the factors of the preceding formula can be readily calculated except the term $B_2{}^2G_2$. This term, when calculated based upon a known machine and its output torque, is almost as large as $B_1{}^2G_1$. This requires both of these terms ($B_1{}^2G_1$ and $B_2{}^2G_2$) to be calculated with a high degree of accuracy for satisfactory results. A process of iteration between calculation and testing has increased the accuracy of calculation until excellent agreement can be obtained between calculation and testing within the tested tooth sizes.

Additional testing has been performed with larger tooth sizes and the data obtained has been factored into the calculation method. The main purpose of this additional testing was to evaluate the effective radius of the tooth corner due to local saturation at the corner. The basic method of calculation is to determine the effective gap (G_2), with the above corner radiused by a method of superpositioning, and then calculate the associated flux density (B_2) from the applied ampere turns at this location. This additional testing with the larger tooth size not only improved the calculation method, but justified the results from the preliminary calculations for the purpose of actuator selection for the 5-kwe system reflector drive.

There is a direct relationship between step size and the number of teeth on the rotor; this relationship determines the rotor diameter. With an outer actuator diameter limitation, the rotor diameter affects the room available for magnetic shell material, stator poles and magnet coil. For each tooth size and step size there is a different performance curve.

Calculations were initially made to arrive at a stepper motor design with a fixed length, shell diameter, and magnetic gap. These calculations were intended to establish the overall performance range and to determine the optimum performance for each available step size, recognizing that the teeth/pole must be an integer, and that the rotor teeth must be two greater than the total stator teeth.

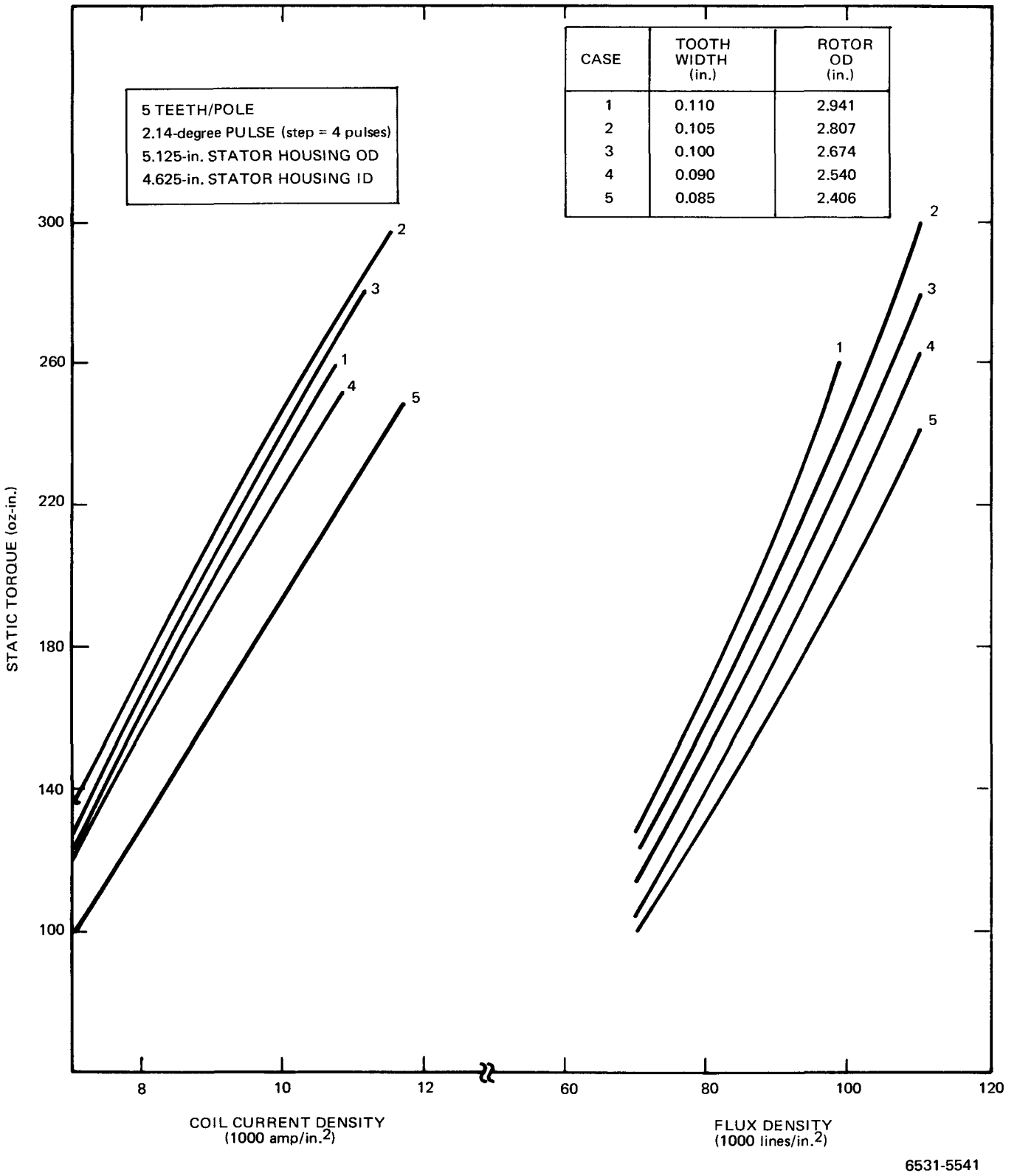

Figure 11. Actuator Static Output

As previously mentioned, the calculations were performed using a computer code which was available prior to the testing of the larger teeth. For the purpose of actuator selection, this code had the following inputs and outputs:

Inputs	Outputs
Trial rotor diameter	Final rotor diameter
Magnetic gap	Teeth/pole
Core length	Coil current
Shell ID	Coil voltage
Shell OD	Current density
Tooth size	Static torque
Slot depth	Stepping torque
Pole width	Turns/coil
Pole thickness	Inductance
Wire diameter	Flux densities in all parts
Conductor resistivity	Ampere turns in all parts

A typical computed torque output, for 5 teeth/pole, 2.143-degree step, is shown in Figure 11. All of these cases are actuators that have the same outside diameter and produce the same step size. As shown in this figure, Case 2 has the best performance at any value of current density. A replot of the variation of torque with tooth size at 8000 amp/in.^{2} in the coil is shown as Figure 12. Therefore, the only actuator to be considered for detail design with this step size containing 5 teeth/pole, would be one with a slot width of about 0.105 in. Similar calculations and curves were made for each available step size (integer slots/pole). This resulted in a finite number of actuators (six) to be evaluated against the requirements.

As the capabilities of the actuator vary for each step size, so do the reflector drive requirements vary. The preliminary torque requirements for the actuator are given in Table 3.

These requirements of actuator torque were obtained by a drive study in which each step size (teeth/pole) was considered, along with the gearing to produce a reference reflector motion for all of the physical environmental conditions and with the feasible range of bearing friction. The expected friction coefficient was 0.35 over the operating range but test data indicated that the friction coefficient has upper and lower limits of 0.60 and 0.10. For the three coefficients of friction, and for each step size, the torque requirements of the actuator were calculated; the resultant maximum torque

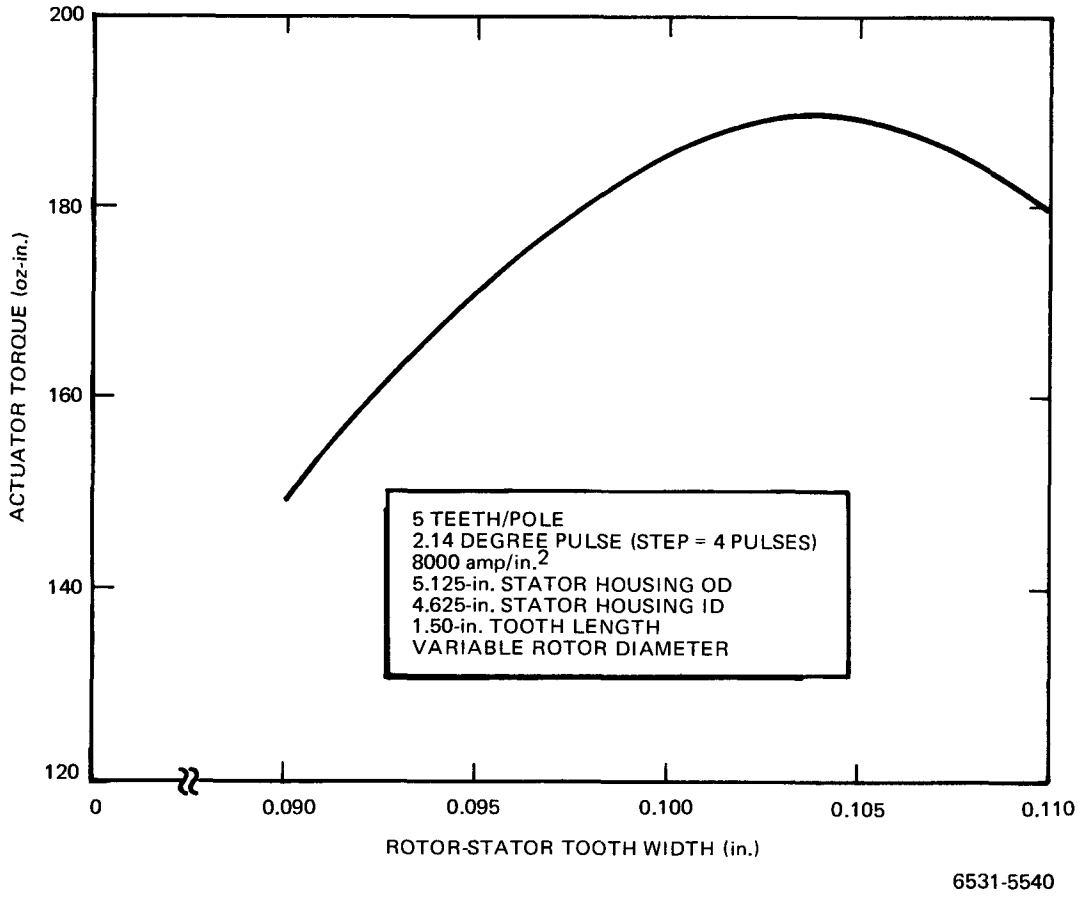

Figure 12. Actuator Torque Versus Tooth Width

TABLE 3

ACTUATOR STEP SIZE VERSUS TORQUE REQUIREMENTS

Teeth/Pole	8	6	5	4	3
Step (deg)	1.37	1.8	2.14	2.65	3.46
Four-step sequence (deg)	5.48	7.2	8.65	10.60	13.84
Reference movement (in.)	0.0054	0.0054	0.0054	0.0054	0.0054
Scram rpm	4.57	6.00	7.12	8.84	11.50
Required step torque, maximum (oz-in.)	103	75	62	49	37
Required scram torque, maximum (oz-in.)	70	51	42	34	27

requirements are listed in Table 3. A typical tabulation of these calculations as performed on the 6-tooth/pole (1.8-degree step) actuator is given in Table 4.

TABLE 4

ACTUATOR TORQUE REQUIREMENTS

Condition	Friction Coefficient		
	0.1	0.35	0.6
Ground test (reactor down)			
Acceleration (g)	+1.0	+1.0	+1.0
Stepping torque (oz-in.)	16.4	42.2	74.4
Scram torque (oz-in.)	9.4	27.2	50.6
Brake holding torque (oz-in.)	3.6	0	0
Flight			
Acceleration (g)	+0.1	+0.1	+0.1
Stepping torque (oz-in.)	3.9	9.9	17.3
Scram torque (oz-in.)	0.1	1.8	6.5
Brake holding torque (oz-in.)	1.1	0.0	0.0
Flight			
Acceleration (g)	-0.1	-0.1	-0.1
Stepping torque (oz-in.)	9.9	24.9	43.9
Scram torque (oz-in.)	0.0	3.7	15.2
Brake holding torque (oz-in.)	3.2	0.0	0.0
Launch (reactor down)			
Acceleration (g)	+16.25	+16.25	+16.25
Brake holding torque (oz-in.)	138.9	0	0
Launch (reactor up)			
Acceleration (g)	-16.25	-16.25	-16.25
Brake holding torque (oz-in.)*	170.8	0	0

*Control Sector held by mechanical full-out stop.

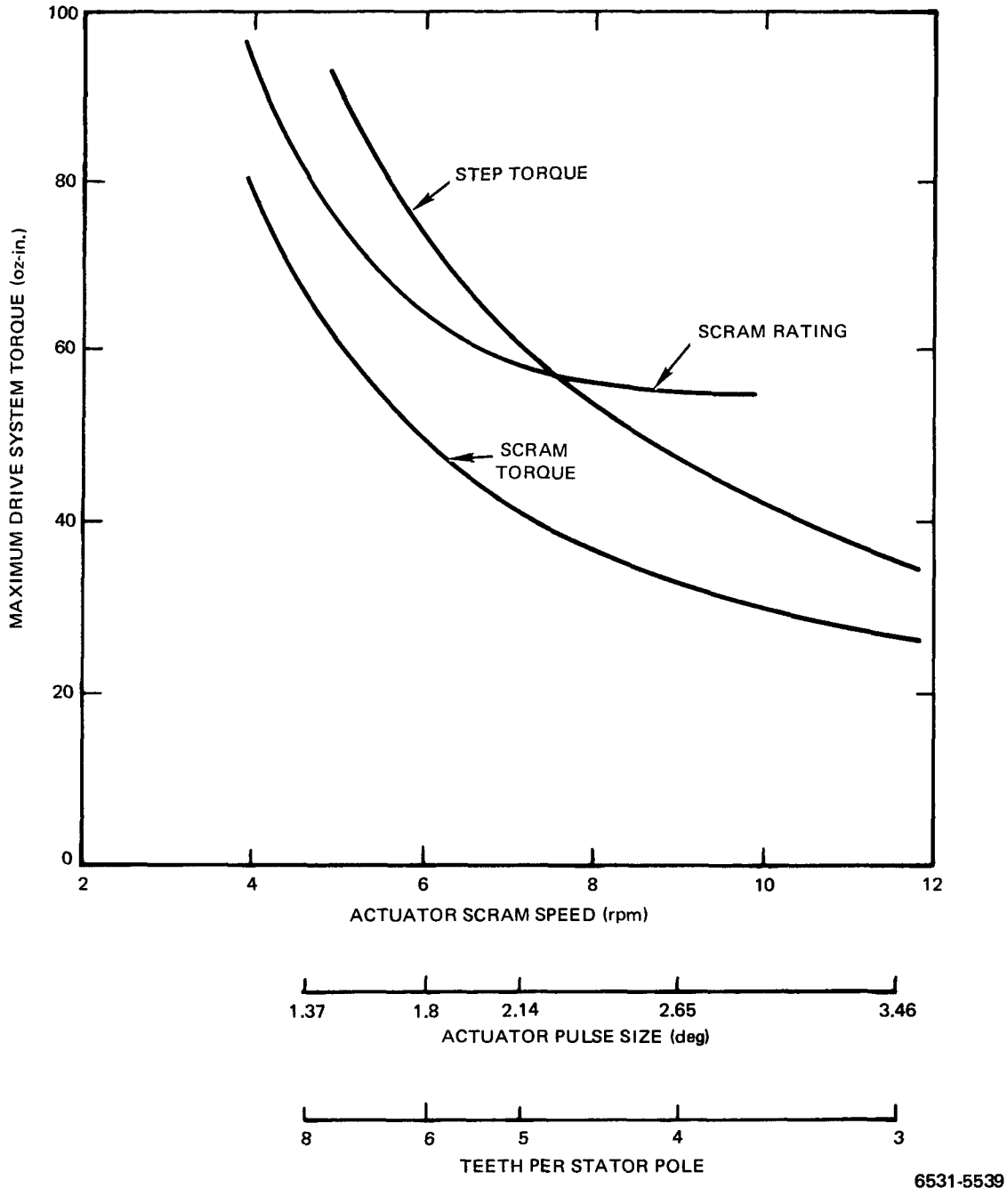

Figure 13. Stepping and Scram Torque Requirements (Ground Test Conditions, Friction Coefficient = 0.60)

The resultant requirements are plotted as Figure 13. Also shown in Figure 13 is a scram rating curve. This is the scram torque curve as modified (by dividing) by the actuator speed derating factor for the various scram speeds as determined from experimental data generated on the S8DR design actuators. As the actuator speed is increased, the time available for phase energization must be decreased. Due to the coil inductance and actuator dynamic characteristics, a less favorable condition for the generation of torque to start the actuator at higher speed results. Commercial units normally start at reduced speed and gradually increase speed for full-speed driving. At scram speeds less than 8 rpm, it is more desirable to apply the derating factor to the actuator than to complicate the controller for variable speed.

There is a difference in the drive systems torque (Figure 13) and the previously discussed peak actuator torque. The peak actuator torque discussed was based upon the torque generated at the maximum permeance change location, i.e., when the rotor is displaced 1/4 tooth pitch. With the rotor so displaced, as by a steady load, the energization of the second phase results in a displacement of that phase of 1/2 tooth pitch, which is a zero-torque location. Therefore, when a steady load is advanced, the rotor must move from the maximum torque location to a location where it may be picked up by the next phase energized. This torque, which is the system stepping torque or dynamic torque, is approximately 63% of the static or maximum phase torque, depending on stepping rate and phase overlap. The result of this calculation is shown in Figure 14, which compares the actuator output capabilities range to the drive torque range for all feasible actuators through the actuator scram speed range, considering all factors of the drive.

On the basis of the preceding evaluation, an actuator having 6 teeth/pole, which results in a 6 rpm scram speed, was the preliminary selection. Then the other parameters are also fixed.

2. Experimental

A minor amount of experimental effort was performed on the 5-kwe system actuator design. The experimental effort consisted of (1) an EM torque test, (2) a sheathed cable termination mockup, and (3) tests of the sheathed cable. The EM torque test was performed to obtain experimental data of the

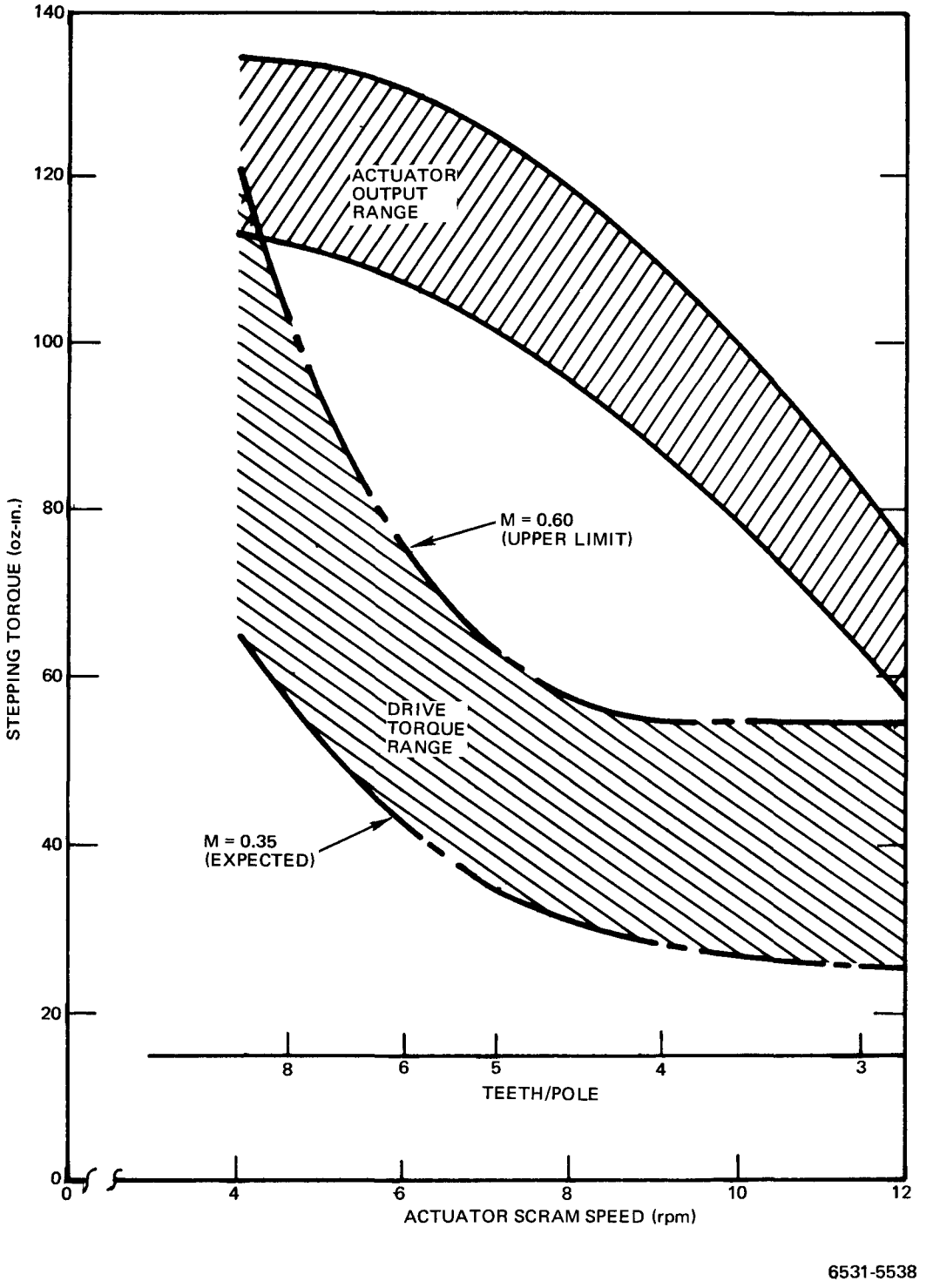

Figure 14. Actuator Output Torque Versus Speed Characteristics

performance of teeth larger than 0.063 in. wide. The sheathed cable termination mockup was an experimental setup to determine the feasibility of the termination scheme and identify fabrication difficulties. Experimental tests of the sheathed cable were performed to determine the cable characteristics. These tests were conducted primarily to aid in the reflector configuration design, but since the end of the cable would have been anchored on the actuator, the results would have some applicability to the actuator design.

3. Design Selection

As previously described, the preliminary design selected was a 6-tooth/pole, 1.8-degree step actuator. Using the experimental data, the larger tooth size test results were factored into the computer program without appreciable change in calculated results. The computer program indicated that a 0.090-in. tooth was as satisafactory as the 0.085-in. tooth previously selected. However, since the smaller rotor of the 0.085-in. tooth was more desirable, due to the greater available coil space, the selected design utilized the 0.085-in. wide teeth. This actuator will meet the output performance of:

Output step size	100 oz-in., minimum
Scram torque (6 rpm)	70 oz-in., minimum
Brake holding torque	180 oz-in., minimum

The brake holding torque is obtained from the engagement of teeth in the tooth brake disk with slots in the tooth brake ring. This toothed brake disk and ring concept is the design used in the S8DR actuator. The brake was sized from the layout and calculated directly, utilizing all the available space. The required axial force to keep the brake disk and ring engaged and to develop the restraining torque was calculated and built into the bellows assembly which restrains the rotational force. The brake was not optimized but designed to be compatible with the stepper motor.

C. PROTOTYPE DESIGN

A layout was prepared incorporating the above design points (see Figure 10). The overall size of the actuator is 5-1/8 in. in diameter and 5-1/8 in. long, (including the first stage of gearing.) This actuator is designed for face mounting, having tapped holes in the front end bell for bolts from the reflector drive

housing. As can be observed, the brake is built into the actuator in a manner similar to the S8DR design, except that the spring action of the brake is included in the bellows assembly design.

1. Description

The actuator, as designed for the 5-kwe Thermoelectric System, consists of three basic parts: the brake assembly, the stepper assembly, and the first stage of gearing. These basic parts all share a common housing alignment and common bearing alignment. The general material of construction is 27% cobalt iron, chosen for its high temperature magnetic capability. The design is fully integrated, avoiding any duplication of function.

The output shaft has both a groove and through-hole for interfacing with the reflector drive rotatable screw shaft. This shaft is integral with the first-stage reduction gear which is made of Hastelloy for strength and its coefficient of expansion match with the cobalt iron. The pinion of the reduction gear is machined into the rotor, which has 50 teeth in its outer diameter (2.706 in.) matching the teeth of the pole faces. The rotor and poles are machined from cobalt iron selected for its magnetic properties at high temperature.

The stator has a 4-phase, 8-pole dc winding which, with the rotor design, causes the rotor to rotate 1.8 degrees for each sequential pole energization. The stator windings utilize a stainless clad copper conductor with "E" glass as turn-to-turn insulation on the coils, which are wound on alumina bobbins prior to being mounted on the poles. Electrical connections are made with AWG No. 22 stranded conductor insulated with woven "S" glass.

A rotating brake disk is threaded on the end of the rotor shaft and is accurately positioned by means of a conical fit. Matching slots and teeth are machined in the outer diameter of the rotating brake and the stationary brake ring so that the two rings, when engaged, will lock together preventing rotation. Both brake parts are made from cobalt iron: the brake disk to match the coefficient of expansion of the rotor, and the brake ring because it is the armature of the magnetic brake.

Brake reaction forces are carried through the bellows assembly, which also acts as the brake ring compression spring. This assembly is located and pinned

so that the slots and teeth in the brake disk and brake ring are aligned when phases A or C are energized. Energization of the brake coil pulls the stationary brake ring (armature) to the brake pole faces, against the spring of the bellows, releasing the shaft to rotate to a new position, based upon the energization of sequential poles in the stepper. The material of construction of the bellows is Inconel, chosen for its high-temperature mechanical properties.

The bearings of the actuator are carbon graphite in which alumina journals rotate. Two sizes of bearings are employed in the design. The output bearings are identical and are sized for the load, while the rotor bearings are oversized to allow the pinion cut into the rotor to pass through the bearing. This preserves the one-piece rotor construction. The use of identical sized bearings on a shaft facilitates the fabrication of the assemblies. Thrust washers are located on each side of the inboard bearing to accurately locate the shaft for both gear and brake operation.

All other materials of construction, i.e., brake poles, end bells, outer housing, etc., are made from cobalt iron, either because of its flux-carrying requirement or a requirement to match the coefficient of expansion of a flux-carrying part.

2. Expected Performance

The performance of an actuator is not only dependent upon the physical design, and materials used, but also upon the supplied power (voltage and current) and the phase overlap as successive phases are energized. The need of phase overlap can be visualized by considering that if a phase should come on late, the rotor would be free to rotate under load torques during the time none of the phases were energized. Tests were performed on the S8DS actuator to evaluate the effect of overlap on the actuator performance. It was determined that the full advantage of overlap was obtained with 5 msec overlap and additional overlap was of no advantage. Therefore, the expected performance must be based upon the expected supplied power condition. The performance expected from the calculated 5-kwe system actuator is listed at the phase overlap and current density used on the S8DS actuator (5 msec overlap, 200 msec minimum pulse width, 8,666 amp/in.^{2} stator conductor current density, and 2743 amp/in.^{2}

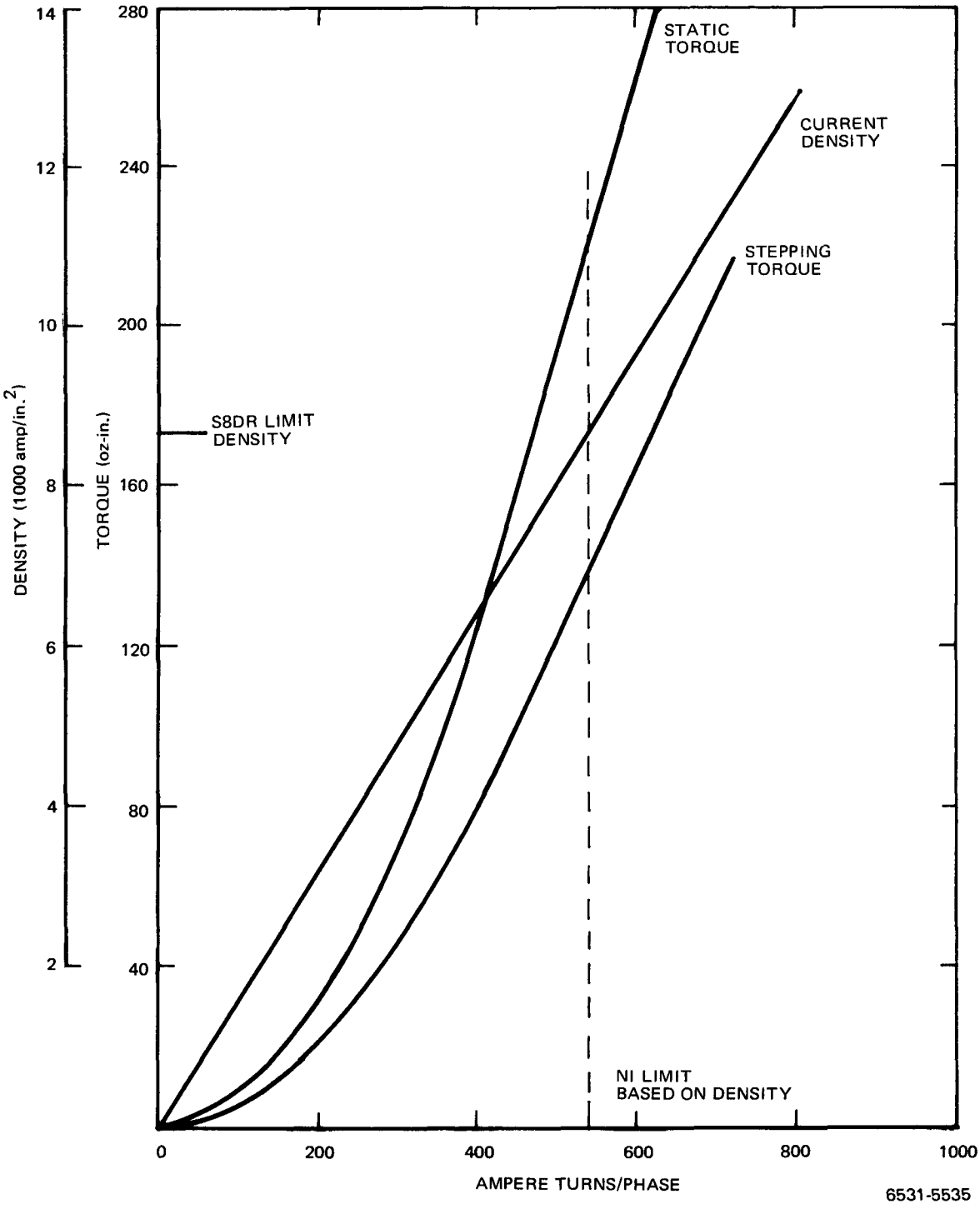

Figure 15. Calculated Performance Versus Ampere Turns Per Phase Actuator 5-kwe Thermoelectric System

brake coil current density). From the calculations presented in Section C-3, the expected actuator performance is as listed in Table 5.

TABLE 5

EXPECTED ACTUATOR PERFORMANCE

Item	Expected	Required
Static torque (oz-in.)	223	
Stepping torque (oz-in.)	140	100
Scram torque (oz-in.)	105	70
Holding torque (oz-in.)	225	180

The calculated performance curve is shown in Figure 15.

Shock, vibration, and acceleration requirements are not expected to be a problem. The S8DR actuator (Dev. 010) was successfully tested to three times the acceptance level, based on the Saturn V launch load. This is expected to be more severe than the requirements of the 5-kwe system actuator. Since the 5-kwe actuator is basically (due to larger bearings, shaft, and radius, as well as a very short shaft length) a more shock- and vibration-resistant design configuration than the S8DS actuator, no difficulty is expected from these environmental requirements (shock, vibration, and handling). Although the required life of the 5-kwe system actuator is relatively long (44,000 hr) no difficulty is expected in achieving this life requirement as the operational temperature and rotational requirements are low when compared to the S8DR testing. Extensive thermal test data has been obtained on S8DR actuators at thermal transient rates which exceed those expected to exist in the 5-kwe system.

3. Design Analysis

The design analysis is presented in two parts, electromagnetic, and mechanical.

a. Electromagnetic

(1) Stepper Motor

The basic stepper electromagnetic calculations were performed on a computer program. The input to the program is the physical size associated with

the stepper motor. The magnetic material constants are built into the program for cobalt iron at elevated temperature. The program inputs are:

DR = trial rotor diameter (in.)
G = magnetic gap (in.)
CL = length of teeth (in.)
DS = diameter of stator ID (in.)
SD = slot depth (in.)
OD = outside diameter (in.)
PW = pole width (in.)
PL = pole length (in.)
WD = wire diameter (in.)
BWD = bare wire diameter (in.)
TW = tooth width (in.)
RC = resistivity of conductor (ohm-in.)

The output is listed in two sections. Section 1 is the listing of the machine constants as follows:

Final rotor diameter
Teeth per pole
Turns per coil
Coil resistance ohms
Teeth on rotor
Step size degrees
Actuator inertia

The second section is the performance for incremental gap fluxes from 20,000 lines/in.^{2} until the program is terminated by one of the built-in stops. For each flux density, the listed output is as follows:

Gap flux
Coil current
Coil voltage
Coil current density
Static torque
Dynamic torque
Coil inductance
NI/pole

In addition, each set of readout data has a set of diagnostic readout data for detailed evaluation of individual elements, such as flux densities, ampere turns, areas, etc. Figure 15, as previously mentioned, is the plot of the calculated performance for the selected 5-kwe system actuator. At the expected operating point, all values of electromagnetic parameters are similar to the S8DR values. The final current density is identical to the S8DR density. The following listing is a summary of the electrical and electromagnetic design:

Magnetic

Ampere Turns (NI)	
Gap	440
Pole	31
Shell	49
Teeth	7
Rotor	13
Total	540

Flux Densities (1000 lines/in.^{2})	
Gap	88
Pole	85
Rotor	47
Shell	43

Saturation factor $\frac{540}{440} = 1.23$

Coil and Connections

Turns/coil	98
Wire size	24 AWG
Input Phase Current	5.5 amp
Connection	2 parallel coils/phase
Current density	8,666 amp/in.^{2}

Torques (oz-in.)

Expected static	223
Expected stepping	223 x 0.63 = 140
Scram speed derating	0.75
Expected scram	140 x 0.75 = 105

(2) EM Brake

The EM brake is of the flat face design as was the brake in the S8DS actuator. Again, a computer program has been set up, but for the computational assistance rather than for providing a detailed design. The computer program accepts the physical size of the brake configuration and computes the required coil input and force generated for incremental values of flux density at the inner pole. The magnetic material constants are entered into the program and are for cobalt iron at elevated temperature. The method of computation

is to input into the program the physical size, and calculate the force and coil requirements for various flux densities. For each magnetic gap so calculated, the force at the S8DR brake coil density was determined and plotted as shown in Figure 16. This information was used to plot Figure 17. The basic selected gap is 0.070 or less to provide adequate margin over the requirement of pulling the brake against a 2-1/2-lb spring. The input data are as follows:

SØD	=	shell OD (in.)	AT	=	armature thickness (in.)
SID	=	shell ID (in.)	CBC	=	coil bobbin cavity (in.)
CØD	=	core OD (in.)	PØD	=	pole OD, inner (in.)
CID	=	core ID (in.)	PID	=	pole ID, outer (in.)
TBP	=	thickness back plate (in.)	FMA	=	flux maximum allowable (lines/in.^{2})
TIP	=	thickness inner pole (in.)	G	=	gap magnetic (in.)
TØP	=	thickness outer pole (in.)	BWD	=	bare wire diameter (in.)
AØD	=	armature OD (in.)	WD	=	wire diameter (in.)
AID	=	armature ID (in.)	RC	=	resistivity of conductor (ohm-in.)

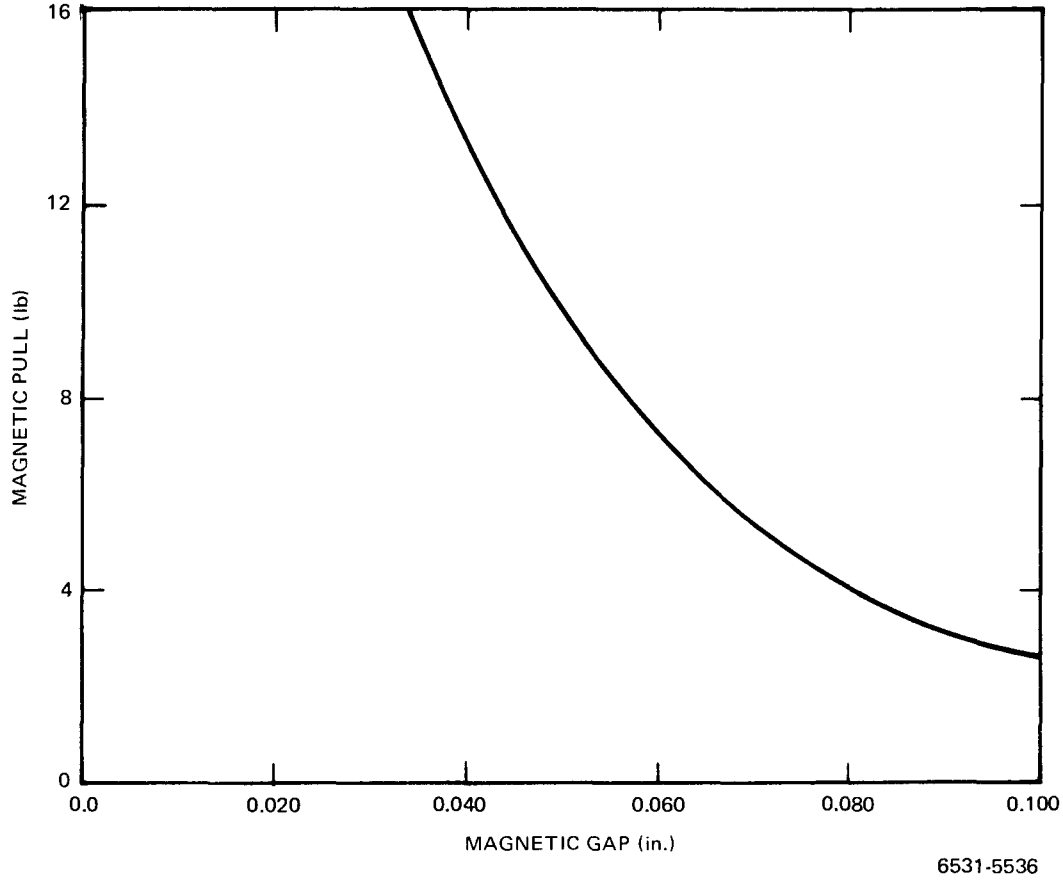

Figure 16. Magnetic Pull vs Magnetic Gap at S8DS Operating Current Density of 2743 amp/in.^{2} (Magnet Cavity 0.600 in., 5.125-in. OD, 330 Turns, No. 24 AWG)

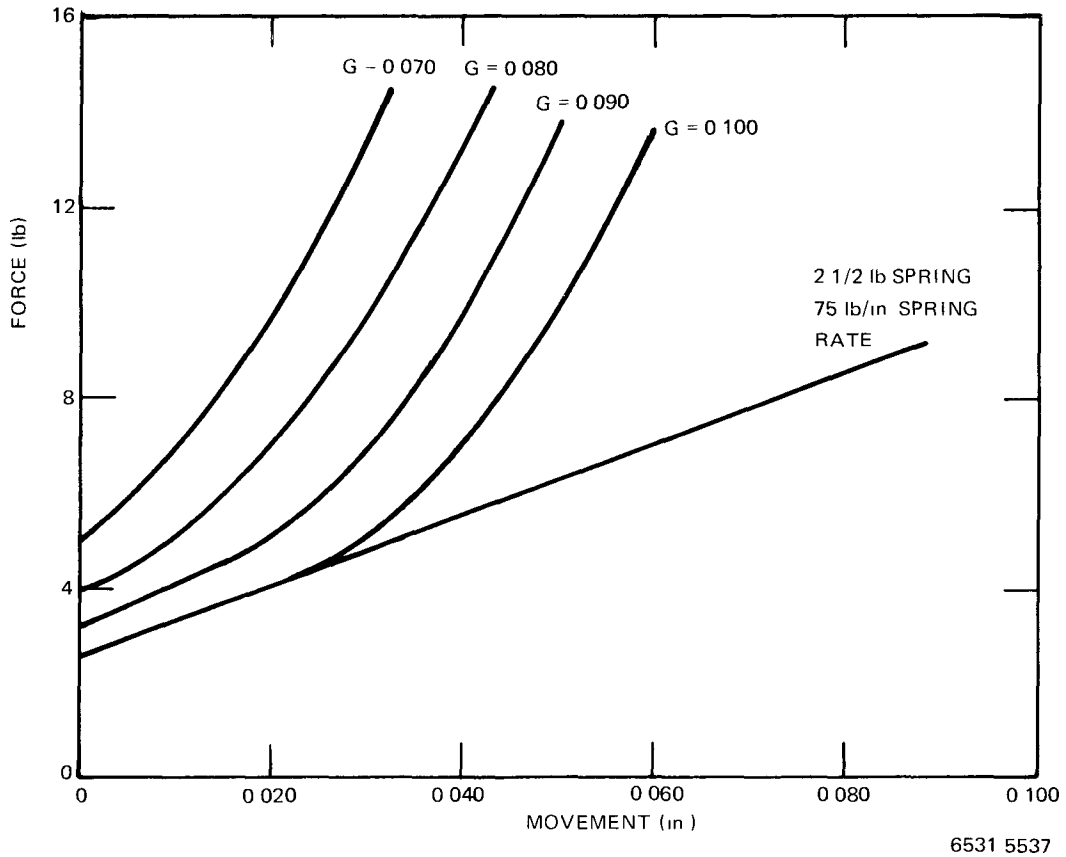

Figure 17. Force vs Movement for Various Gaps at S8DS Operating Current Density of 2743 amp/in.^{2} (Magnet Cavity 0.600 in., 5.125-in. OD, 330 Turns, No. 24 AWG)

The output of the computer program is basically diagnostic data and is in two types of sets: (1) areas, and (2) magnetic densities, ampere turns, etc. For each calculated flux density, there is a printout for that density, total force, coil current, and coil current density from which performance may be calculated.

The following is a list of the electromagnetic design results:

Magnetic

Ampere Turns (NI)	
Inner gap	136.0
Inner pole	1.8
Core	12.7
Back plate	6.3
Shell	7.1
Outer pole	1.3
Outer gap	118.0
Armature	3.6
Total	286.8

Saturation factor = 1.13

Flux Densities (1000 lines/in.^{2})	
Inner gap	6.2
Inner pole	35.8
Core	26.5
Back plate	46.8
Shell	9.6
Outer pole	30.8
Outer gap	5.4
Armature	24.2

Coil and Connections

Turns/coil	330
Wire size	No. 24 AWG oxalloy
Brake Input current	0.869 amp
Connection	single coil
Conductor current density	2743 amp/in.^{2}

Forces and Torques

Magnetic pull	5.0 lb
Resultant magnetic pull	(See Figure 16)
Spring load	2.5 lb
Holding torque	225 oz-in. at μ = 0.1
Spring rate	75 lb/in.
Magnetic gap	0.070 in.

b. Mechanical Calculations

The actuator can be expected to be subjected to both torsional and direct loadings (acceleration, vibration, and shock). Although in the expected reactor launch orientation, the reflector segment would be restrained by pins removing any actuator torsional loading, the mechanical approach was to consider the actuator as restraining its torsional load at the time it was subjected to maximum direct loading. Maximum torsional loading would be that load which could cause the brake to slip. The present brake is designed to slip between 180 and 220 oz-in. of torque, based upon calculations and S8DR testing of the equivalent brake. This approach of combined stresses (direct loading, torsional

loading, and built-in stresses) was applied to each element, or mechanical unit of the design, and the results were compared with the results of the identical calculations performed on the S8DR actuator. These elements will be covered individually as they were calculated.

(1) Bearings

The bearings are sleeves of carbon graphite material installed, with an interference fit, in the end bells. There are two sets of bearings: (1) rotor shaft bearings, and (2) output gear bearings. The detailed calculation indicates that a loading of the bearing due to reaction forces on the shaft tends to slightly reduce the stress levels from the ambient condition. The maximum housing stress (in the rotor bearing) is 11,539 psi, an increase from the S8DS value of 8655 psi, under worst-case conditions. The increased stress is due to the larger diameters. The larger diameters allowed the sleeve stress to decrease to 15,592 from 17,039 psi. The diametral clearances between the bearing and journal were chosen to be held to the S8DR values at ambient temperature and allowed to decrease slightly at elevated temperature, less than 0.00004 in. at the worst case, an insignificant amount.

(2) Bearing Journals

The journals that run in the carbon graphite bearings are alumina coated. The technical approach is mainly empirical and is based upon the proven and tested methods of the S8DR. The initial coating thickness is less than 0.006 in., with a finished thickness of 0.002 to 0.003 in.

(3) Rotor Calculations

The rotor stresses were calculated under the combined load condition. The stresses obtained in the calculations are all very low and adequate strength is indicated. The following is a summation of the stresses:

Location	Stress (psi)		
	Bending	Shear	Principal
Near pinion	588	414	803
Near outboard bearings	3235	1250	3662
Outboard bearing	925	389	1067
Inboard bearing thread relief	382 (torsion)	2277	2476

(4) Gear Calculation

The calculated gear ratio was 2.778. The stresses were calculated by two methods; the highest resultant stress of the gear teeth was 14,029 psi on the pinion and 3502 psi on the gear. Calculations for the attachment loading point (shaft hole) indicate a stress of 530 psi.

(5) Brake Calculations

Calculations for the brake disk and teeth indicate a tooth stress of 840 psi, while the loading on the disk is pessimistically calculated at 3,000 psi.

(6) Critical Frequency

The critical frequency of the assembly is only 8-1/3 Hz, which is well below the frequency expected to be applied to the actuator.

(7) Structural

The only structural assembly analyzed was the end bell containing the thrust bearing. In comparison, all other structures have a much lower loading. This end-bell stress, when stress concentration is included, is only 1782 psi.

(8) Brake Torsional Restraint

This torsional restraint member, which is built like a bellows, has a maximum torsional loading of 33,125 psi and a compressed-state load of 40,000 psi during stepping.

(9) Summary

The results of the mechanical calculations are judged to be satisfactory for the stresses and materials considered (Table 6). Worst-case conditions are listed with the calculated design factors at 800° F; these results are based on the following material capabilities:

Material	Yield (psi at 800° F)
Cobalt iron	30,000
Inconel 718	155,000
Carbon-graphite (compressive)	25,000

TABLE 6

SUMMARY OF MECHANICAL CALCULATIONS

Unit	Stress (psi)	800° F Design Factor
Rotor shaft	3,662	7.19
Rotor pinion	14,029	1.14
End bell	1,782	15.84
Brake teeth	840	34.16
Brake disk	3,000	9.00
Torsional restraint	40,000	3.13
Bearing	17,000	.47

$$\text{Design Factor} = \frac{\text{Yield Stress}}{\text{Load Stress}} - 1.0$$